THESIS

EXPERIMENTAL EVALUATION OF A STANDALONE HOLLOW CATHODE APPARATUS WITH A MAGNETIC FIELD

Submitted by

Emily X. Ku

Department of Mechanical Engineering

In partial fulfillment of the requirements

For the Degree of Master of Science

Colorado State University

Fort Collins, Colorado

Fall 2024

Master's Committee:

Advisor: John Williams

Ciprian Dumitrache
Christopher Thornton

ABSTRACT

EXPERIMENTAL EVALUATION OF A STANDALONE HOLLOW CATHODE APPARATUS WITH A MAGNETIC FIELD

Testing hollow cathode assemblies independently from their use in Hall or gridded ion thrusters offers advantages such as reduced test facility size, lower power requirements, and improved diagnostic access. Standalone tests can reveal important cathode characteristics like ignition time, keeper ignition voltage, tip temperature, and current capability. Replicating the plasma phenomena that occur when a cathode operates within a thruster is challenging but essential, as these phenomena can generate energetic ions that erode cathode and keeper surfaces, limiting thruster lifespan. The primary challenge is to accurately emulate thruster conditions in standalone tests and verify this emulation through comparison with cathode-thruster operations. This thesis presents data on a standalone hollow cathode operated with magnetic fields that emulate those in electric propulsion devices, testing it both without an applied magnetic field and with permanent and solenoidal magnetic fields. Measurements of keeper, anode, and cathode-to-ground voltages were conducted over a range of anode currents and flow rates. At certain conditions, the plasma discharge transitioned to a less stable mode known as plume mode, with higher flow rates shifting this transition to higher anode currents. Introducing a magnetic field decreased the anode current at which this voltage shift occurred. Important findings in this work include: (1) Repeat tests with no magnetic field show that the transition behavior was different from one test to another, indicating that transition behavior may be affected by minute changes in cathode apparatus, or there are significant uncertainties associated with the transition and

(2) Significant hysteresis in plume mode transition was observed when increasing and then decreasing anode current. These two findings along with the deleterious effects of the magnetic field have important implications on cathodes operating with Hall thrusters, which often exhibit large, rapid oscillations in discharge current.

ACKNOWLEDGEMENTS

I would like to extend my heartfelt gratitude to my advisor, Dr. John Williams, for his steady guidance on my research, his vast expertise and experience, and his unwavering support and commitment to my personal growth. I would also like to thank my committee members Dr. Ciprian Dumitrache and Dr. Christopher Thornton for their counsel and advice in my thesis and defense.

A special thanks to Seth Thompson for his direction, mentorship, and compassion during the twists and turns of my research journey, as well as to Casey, Cody, and Shawn Farnell for their consistent and open-hearted support. A great thank you to my other lab mates that have helped me and lent an encouraging shoulder through my journey. A final heartfelt thank you to my friends and family for their unwavering support and strengthening hands, which I treasure more than words can convey.

TABLE OF CONTENTS

CHAPTER 1: INTRODUCTION

A primary challenge of in-space travel is the significant amount of propellant needed for missions with large velocity change requirements. Electric propulsion (EP), through accelerating ions to high velocity via electric fields, provides an attractive solution to reducing propellant mass [1]. The Hall thruster (HT) class of EP devices has risen in popularity with their relatively compact design and high applicability to the in-space propulsion needs of governmental and commercial space entities. A Hall thruster produces thrust by accelerating ions through an electric field, with the ions formed through the bombardment of neutral propellant atoms by electrons. The electrons necessary to seed the propellant ionization process and neutralize the ion current are supplied by a hollow cathode [2]. The same hollow cathode designs used in HTs are also used in gridded ion thrusters (GITs), an alternative type of electric propulsion device. Both types of EP device use magnetic fields to confine the electrons and improve their ability to ionize propellant.

Hollow cathodes have a long history of research and development in academia, industry, and governmental laboratories. However, their small dimensions and drastic differences in plasma properties and neutral gas pressure, both from the interior and through the cathode and keeper orifices to exterior regions, make them difficult to characterize and model. Recent research has been focused on the onset and rapid growth rates of plasma instabilities in the exterior regions just downstream of the cathode and keeper orifices. Such instabilities are responsible for generating high-energy ions that exceed the applied voltages under specific current and flow rate conditions [3]. Numerous efforts both in past and recent years have aimed to improve the understanding of the plasma created in the exterior regions of hollow cathodes to predict how energetic ions are created and how to decrease their energy, thereby minimizing erosion-related

cathode lifetime concerns due to sputtering. An early investigation for a mercury hollow cathode performed by Siegfried and Wilbur in 1978 without an applied magnetic field showed significant changes in the plasma properties downstream of the cathode orifice for different modes of operation [4]. Relatively large probes placed at fixed locations within the interior of their cathode were used; however, they were only biased at voltages near and negative of the floating potential to avoid melting the probes. The probes could not access the area around the cathode orifice, and their anode current was restricted to below 10A. Therefore, there is interest in testing at higher anode currents and developing diagnostics that can characterize the plume at those currents without overheating, such as the probes used in hollow cathode studies by Goebel et al, 2005 [5].

A phenomenon that is often observed in hollow cathodes is the transition from a quiescent, relatively steady mode of operation to a higher-energy, noisier and more oscillatory mode of operation. This mode transition phenomenon is referred to by different names in literature, such as ”spot” to ”plume”, or ”quiescent” to ”noisy,” and is theorized to be a result of the downstream cathode region being starved of neutral atoms [6]. Operation in the "plume" mode often results in the production of more energetic ions and higher electron temperatures, which increases the erosion rate of cathode surfaces and reduces cathode lifetime, making it an unfavorable mode of operation [7].

CHAPTER 2: MOTIVATION

While Hall thruster testing requires the inclusion of a hollow cathode, hollow cathodes are often also tested independently from a thruster for many reasons. For example, hollow cathodes tests can be carried out in smaller test facilities with lower pumping speed and only require a fraction of the power and flowrate needed by full thruster tests. Moreover, standalone cathode test configurations typically offer better diagnostic access to the cathode and enable simultaneous cathode development activities alongside thruster development [3, 8, 9]. Although the hope is that standalone tests emulate thruster tests, the differences between the two are not fully documented. In our opinion, a consensus in the EP research and development community has not yet been reached regarding the best configuration and protocol for performing standalone tests.

Many early tests of hollow cathodes were conducted without an applied magnetic field, making it difficult to compare standalone test data with that of a full thruster where magnetic fields are used. Furthermore, experiments have shown that applying a magnetic field to a standalone cathode test can affect its operation and visual appearance. For example, Hall et al, 2019, showed that increasing the magnetic field strength of an HT simulator in a standalone cathode test increases the high-voltage ion content, which can result in increased material sputtering [9]. Additionally, a major life-limiting factor of a magnetically shielded HT is the erosion of the front pole by energetic ions [10] that the cathode might play a role in producing.

It was found that as flow rate was decreased in hollow cathode tests with a magnetic field, the cathode ion energy spectra shifted to higher energies [9]. In subsequent tests, Hall et al, 2021, observed that changes in background pressure have a greater effect on thruster tests than on standalone cathode tests, which has not yet been fully explained [11] but would ease test facility requirements on the pumping speed needed for standalone tests. Finally, studies by Lui et al,

1999, and Imaguchi et al, 2021, have also shown that the presence and orientation of a magnetic field strongly affect the excitation rate, ionization rate, and presence of high-energy ions within a standalone cathode test [12, 13].

The objective of this paper is to detail testing done with a standalone cathode test setup using several magnetic field configurations, one of which closely emulates the field created near the cathode in a gridded ion thruster (GIT) and another that emulates the field created near a cathode positioned on the centerline of a 1.5 kW Hall thruster. Diagnostics are mounted downstream to measure plasma potential and ion energy distribution functions with different cathode flow rates and anode currents. The data collected with these diagnostics, along with the measurement of voltages and currents, are analyzed to document transition behavior from the aforementioned "spot" to "plume" modes. It is recommended that future comparisons be made between standalone tests and those performed with thrusters to develop standalone-cathode test protocols that will effectively validate test results that can guide cathode and thruster development efforts.

CHAPTER 3: EXPERIMENTAL APPARATUS AND PROCEDURE

The experiments described in this paper are carried out at the Center for Electric Propulsion and Plasma Engineering (CEPPE) at Colorado State University (CSU) in a 61-cm diameter, water-cooled vacuum test facility with argon as the propellant. Not only is argon less expensive, but its lower molecular weight compared to krypton and xenon makes ionization more challenging. This property can make it easier to detect issues with standalone cathode tests. In general, higher argon flow rates are required to maintain cathode operation in a quiescent mode compared to krypton or xenon flow rates. A 6.4-mm diameter, instant start hollow cathode with an open keeper design was used for testing, with a 100-mm outer diameter stainless steel anode positioned 35-mm downstream of the cathode orifice. Both a permanent ring magnet and a solenoidal magnet were used to simulate the magnetic fields of a GIT and HT, respectively. Photographs of the experimental apparatus with both magnetic field configurations are shown in Figure 1, and Figure 2 shows electrical and gas feed line schematics.

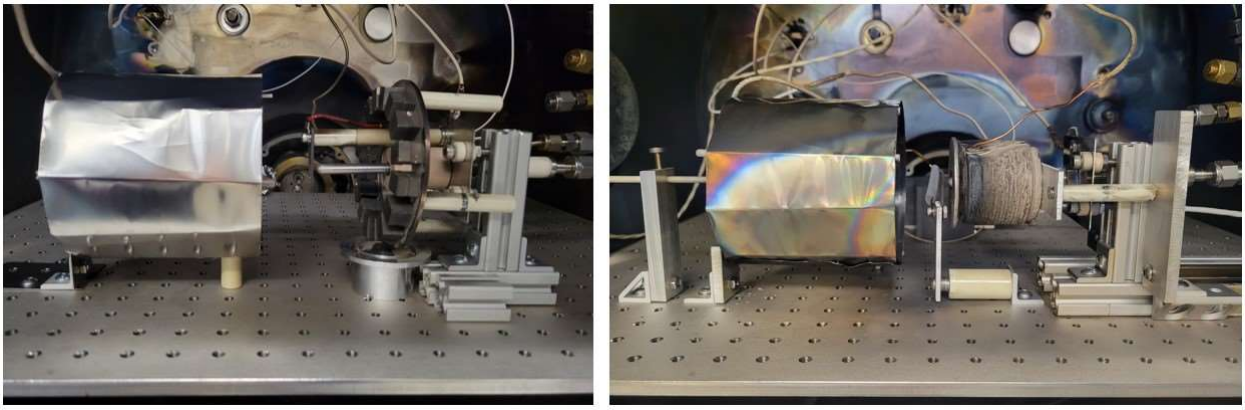

Figure 1: Standalone cathode test setup in a CSU vacuum chamber, with permanent (left) and solenoidal (right) magnetic field simulators

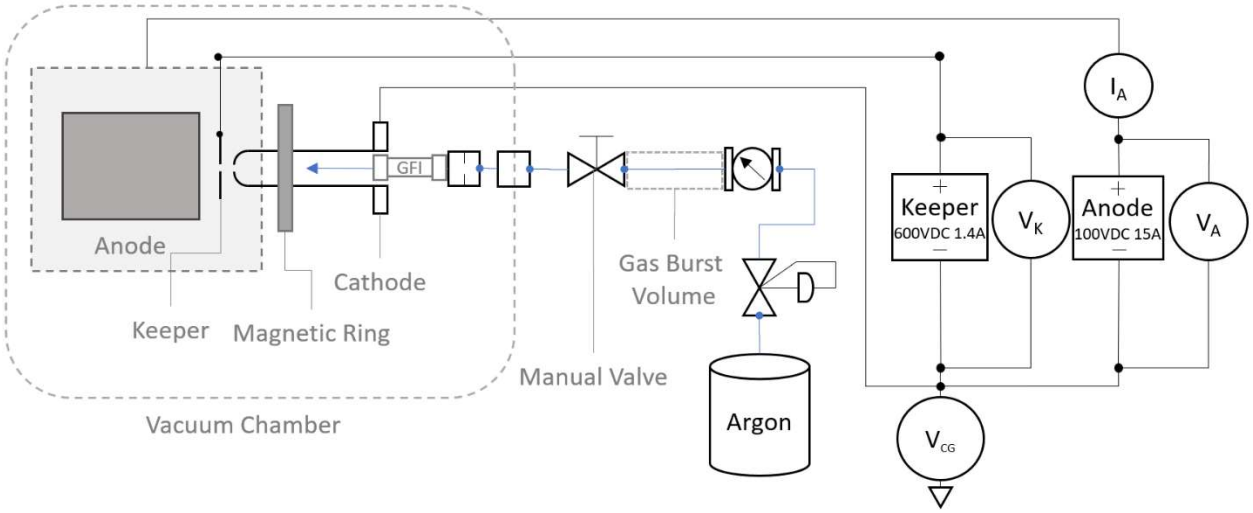

Figure 2: Cathode test apparatus schematic

Section 3.1 Permanent and Solenoidal Magnet Simulators

A 100-mm outer diameter annular ring holding 28 Samarium Cobalt (SmCo) permanent magnets is used to simulate a permanent magnetic field produced near a hollow cathode in the main discharge of a GIT, while a center coil assembly from a 1.5 kW HT was used to simulate a solenoidal magnetic field. The radial and axial magnetic field strengths were mapped using a magnetic field mapper while the coils of the solenoid were operated at a current of 10A. Figure 3 shows the radial magnetic field contours, which are quite symmetric about the centerline of the coil, suggesting good uniformity. In this plot, Y is the axial position and X is the radial position, and the cathode tip is positioned near the coil's origin with the cylindrical anode entrance positioned at Y = -35 mm. The axial magnetic fields measured on the centerline of the coil and permanent magnet configurations are shown in Figure 4, with the position at 0 mm representing the front face of the permanent magnets and center coil, respectively. While the cathode position remained fixed with the solenoidal magnetic field configuration, it was moved along the axis in the permanent magnet tests. The anode entrance is always located 35 mm downstream from the

cathode orifice in the tests described in this thesis, or, in other words, the permanent magnet ring was moved in the axial direction relative to the origin location shown in Figure 4a while the anode (at Y= -65 mm in this plot) and the cathode (at Y= -30 mm in this plot) were held at fixed axial locations. The peak axial field referred to in the sections below is the peak occurring at about Y= -30 mm. In the solenoidal coil tests, the cathode tip was positioned a few millimeters downstream of the coil face at the peak field location.

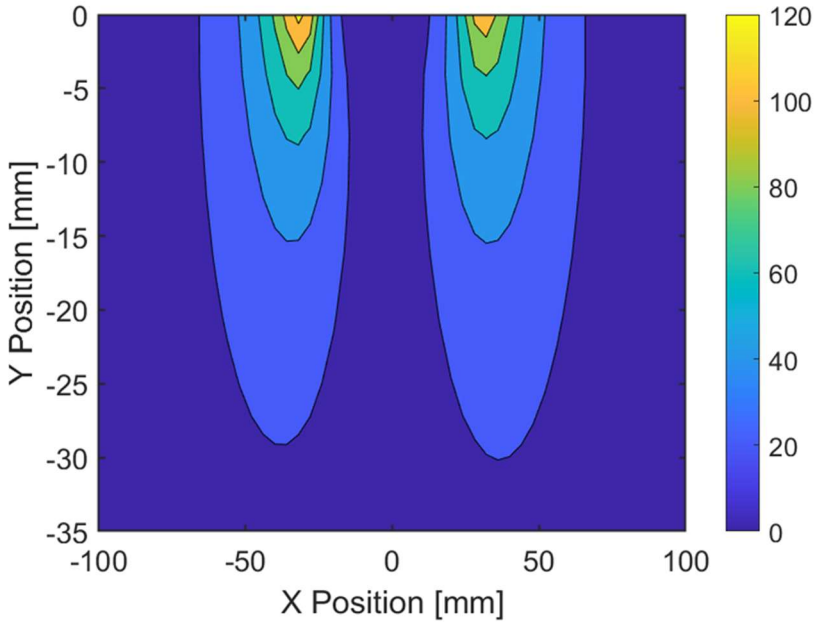

Figure 3: Solenoidal center coil radial magnetic field strength in Gauss

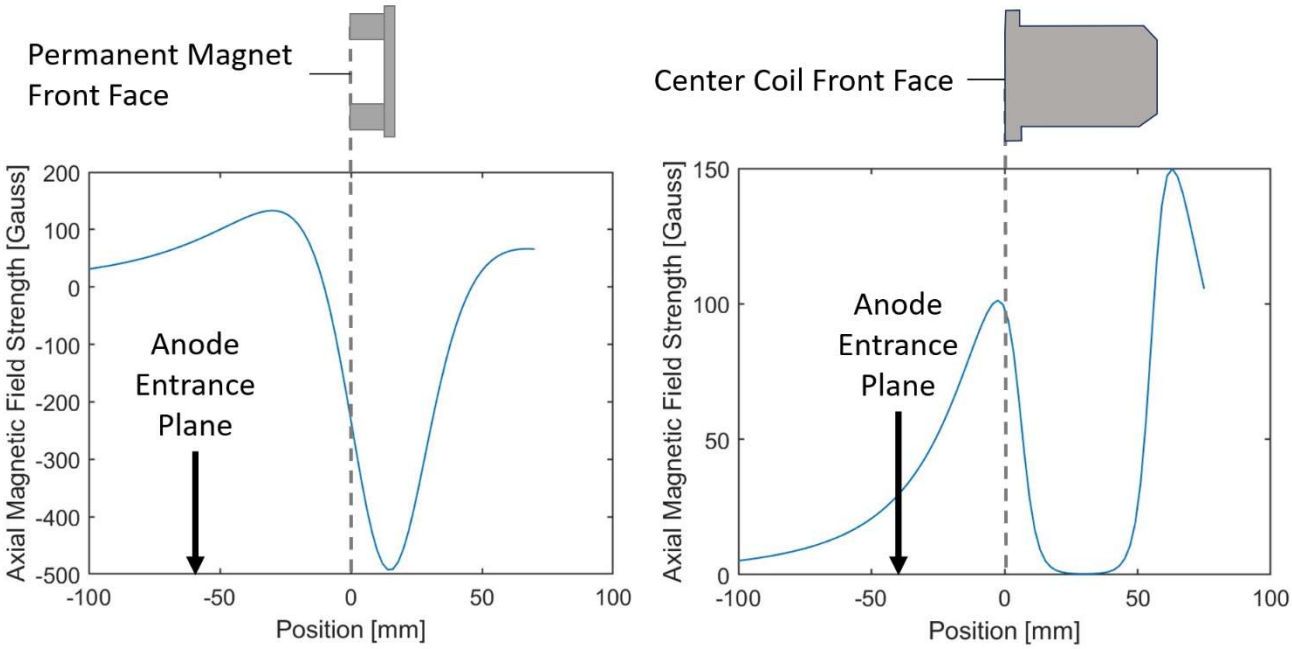

Figure 4: Axial magnetic field strength of permanent (left) and solenoidal (right) magnetic field simulators

Section 3.2 Diagnostics and Data Acquisition

An emissive probe made from a 12 mm long, 76 μm diameter tungsten wire, was placed on the centerline at 67 mm downstream of the cathode orifice and used to measure the plasma potential within the anode and study the association of plasma potential with the imposed anode current and cathode flowrate operating condition. The filament heating current for making plasma potential measurements was found to be around 3A, and both hot and cold probe floating potentials were taken at each current and flowrate operating point. A retarding potential analyzer (RPA) was mounted perpendicular to the cathode axis at the axial location of the cathode tip and 6-cm radially from the centerline. The RPA was used to measure the ion energy distribution of the ions flowing radially away from the cathode-anode region. Nearly all the data discussed below were taken with a data acquisition system to streamline tests, and only a handful of tests were performed using manual data recording.

Section 3.3 Experimental Procedure

Before every experiment, the vacuum chamber is pumped down to a pressure of 10^{-5} Torr and the heaterless cathode is started using a fixed volume release procedure defined by Ham et al [14]. The cathode is operated at a nominal condition of 2A of anode current and 10 sccm Ar flow through the cathode for an hour prior to data collection. A total of four separate test campaigns were performed, the apparatus and diagnostics of which are shown in Figure 5.

Before discussions of the various test campaign results are made, we mention here that the vacuum chamber used to perform the testing described in this thesis had a relatively low pumping speed. The chamber pressures induced by Ar flow rates from 8 to 20 sccm are shown in Figure 6 and listed in Table 1. At 20 sccm of argon flow, the chamber operates at a pressure of 380 μTorr, which is about 40 times higher than the maximum chamber pressure recommended for Hall thruster testing. Although the chamber pressures are high, we point out that the neutral densities within a few cm of the hollow cathode are similar to neutral densities around cathodes operated with a thruster. We also point out that the mean free path of a ~50-100 eV Ar ion is about 20 cm at the 20 sccm Ar flow condition, which is nearly ten times larger than the distance from the cathode to the anode, emissive probe, and RPA.

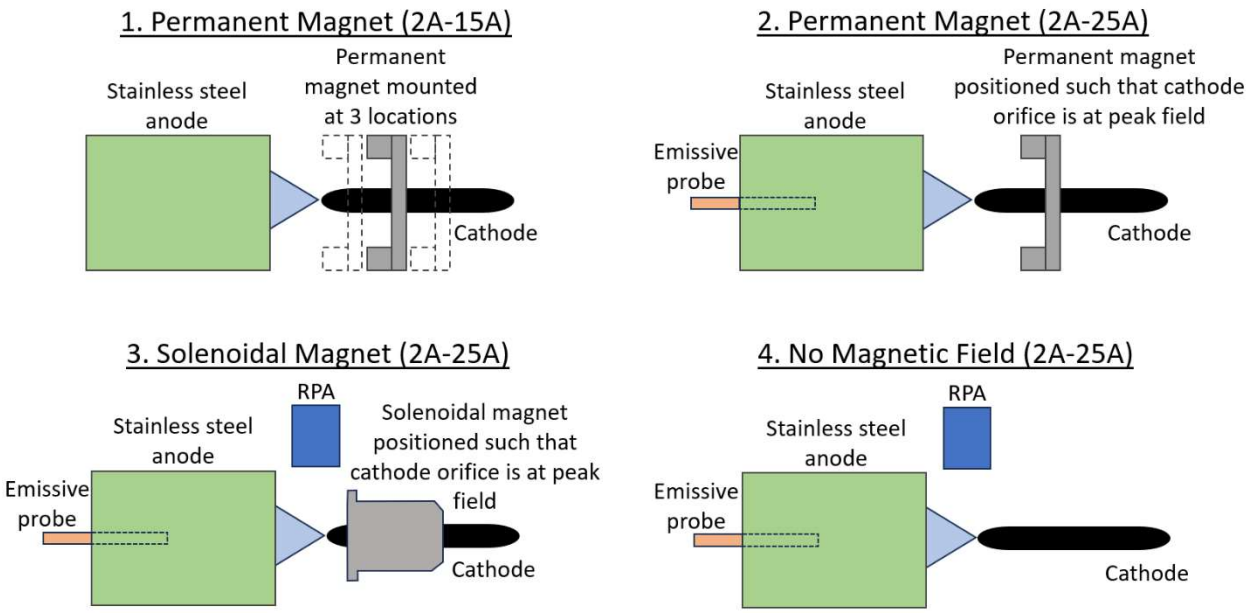

Figure 5: Experimental apparatus and diagnostics for all four experiments performed at anode currents from 2A to 25A

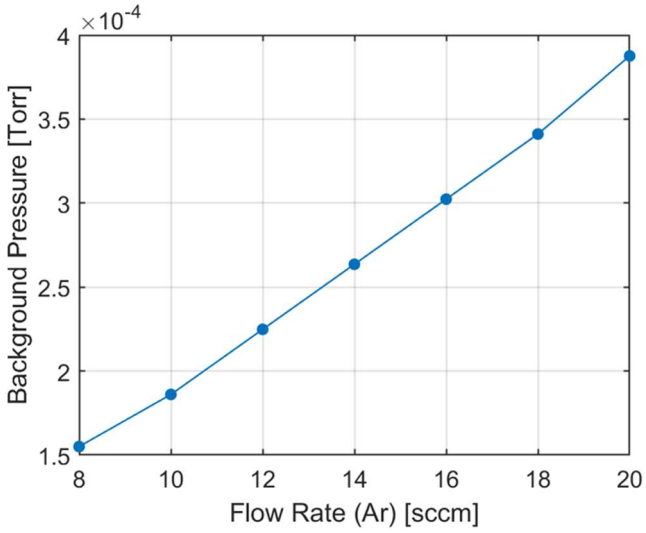

Figure 6: Chamber pressure with respect to Ar flow rate.

Table 1: Chamber pressure at each Ar flow rate tested.

Flow Rate [sccm]	Background Pressure [Torr]
8	$1.55 * 10^{-4}$
10	$1.86 * 10^{-4}$
12	$2.25 * 10^{-4}$

14	$2.64 * 10^{-4}$
16	$3.03 * 10^{-4}$
18	$3.41 * 10^{-4}$
20	$3.88 * 10^{-4}$

Subsection 3.3.1 Permanent Magnet Test Campaign 1 (Anode Currents Ranging from 2A-15A)

During testing with the GIT ring magnet, the cathode flow rate was varied from 8 to 20 sccm in 2 sccm increments, and the DC keeper, anode, and cathode coupling voltages are recorded over a range of anode currents from 2A to 14.5A. Data were taken with 1A increments, with 0.5A increments close to the anode current where the plasma transitions to a strongly luminous mode to better capture where the transition occurs. Oscilloscope traces are also taken at each anode current to study keeper, anode and coupling voltage oscillations. Each test of all the flow rates and anode currents takes about 7 hours to perform to allow adequate time for the cathode to equilibrate between the test conditions.

Data were taken with the GIT-like magnetic field as shown in Figure 5.1: cathode orifice positioned 1 cm downstream of the peak magnetic field, cathode orifice positioned 1 cm upstream of the peak magnetic field, and cathode orifice positioned at the peak magnetic field. These data were compared to data collected with no magnetic field (Figure 5.4).

Subsection 3.3.2 Permanent Magnet Test Campaign 2 (2A-25A)

After initial testing, there was a desire to evaluate higher anode currents as well as make plasma potential measurements within the anode region. Therefore, another round of tests was conducted varying the cathode flow rate from 8 to 20 sccm in 2 sccm increments. The DC keeper voltage, anode voltage, cathode coupling voltage, and plasma potential are recorded over a larger range of anode current: from 2A to 25A. The data acquisition software allowed for automatic sweeping of the power supply; therefore, data were taken in 1A increments in both increasing and decreasing order (i.e., 2A to 25A and then 25A to 2A). The emissive probe heating current

was alternated from 0A to 3A at each operating point to capture the cold and hot probe floating voltages, and oscilloscope traces of keeper voltage, anode voltage, coupling voltage, and anode current were also taken at each operating point. All testing was performed with the cathode tip positioned at the peak magnetic field location.

Subsection 3.3.3 Solenoidal Magnet Test Campaign (2A-25A)

As mentioned above, a heaterless cathode was mounted along the centerline of the solenoidal coil assembly for a 1.5kW HT with the cathode orifice located at the peak magnetic field location. A current of 10A is applied to the coil during testing, and similarly to the other cathode tests, the DC keeper, anode, cathode-to-ground, and plasma potential voltages are taken from flow rates of 8 to 20 sccm and from anode currents of 2 to 25A. An emissive probe is used to capture the plasma potential readings like before, and an RPA was mounted radially to capture the ion energy distribution. Oscilloscope traces were taken at each operating point.

Subsection 3.3.4 No Magnetic Field Test Campaign (2A-25A)

As RPA and emissive probe data had been unavailable for the cathode with no magnetic field tests, another round of tests was performed with the emissive probe and RPA for this test configuration. Data were taken from 8-20sccm flow rates and 2 to 25A anode currents. The emissive probe and RPA were left in the same location used in the coil test configuration. Oscilloscope traces of keeper voltage, anode voltage, coupling voltage, and anode current were also taken at each operating point.

CHAPTER 4: RESULTS

Section 4.1 Comparison of Permanent Magnet and No Magnetic Field Test Campaign Data Sets (2A-15A)

Subsection 4.1.1 No Magnetic Field

The keeper, anode, and cathode coupling voltage with respect to anode current for no simulated magnetic field are shown in Figure 7. It has been observed that at a certain anode current threshold, the cathode transitions to a mode where the plasma is much more luminous throughout the vacuum chamber volume. Initially, we were unsure if the observed change was due to the anode current coupling to the inside surface instead of the outside surface of the anode. Therefore, we modified the anode by placing a floating metal surface around the outside that would prevent current from being collected to this surface. Tests performed after installing the external anode shield showed the same transition to luminous plasma creation as seen in tests without the external anode shield. While no differences were seen between the tests, we opted to leave the external anode shield installed. All tests reported in this thesis were performed with the shield installed.

In the luminous mode, the cathode coupling voltage decreases to more negative values, the anode voltage increases, and the voltage oscillation amplitudes increase. We refer to this plasma discharge state as the plume mode of operation. It is interesting to note that the DC keeper voltage is not noticeably affected by the transition, suggesting that the plume mode transition is not caused by drastic changes to the plasma conditions within the hollow cathode interior, within the cathode orifice, or between the keeper and cathode orifices. Another interesting point is that the cathode-to-ground voltage slowly increases as the anode current is increased from 2A until it is slightly positive of the vacuum chamber ground before dropping negative at the transition

point and at anode currents above the transition point. Although this behavior is inconsistent with the observation that cathode coupling voltage is always negative of ground when a cathode is tested with a thruster, it is an interesting finding that might help researchers identify when cathode operational conditions are on the threshold of transitioning the cathode operation into the plume mode. We are currently unaware of any standalone cathode studies that float the cathode-keeper-anode circuits with respect to the vacuum chamber ground or studies that do this and report the cathode-to-ground voltage as we are doing. All the studies we know about electrically ground the cathode to the vacuum chamber. The anode voltage and cathode-to-ground voltage graphs in Figure 7 show that the mode transition happens at lower currents when the flowrate is lowered. It is expected that an anode current transition point will also happen with an applied magnetic field, but some studies do not report large changes in plasma luminosity when applied magnetic fields are present [9]. Application of magnetic fields is discussed next.

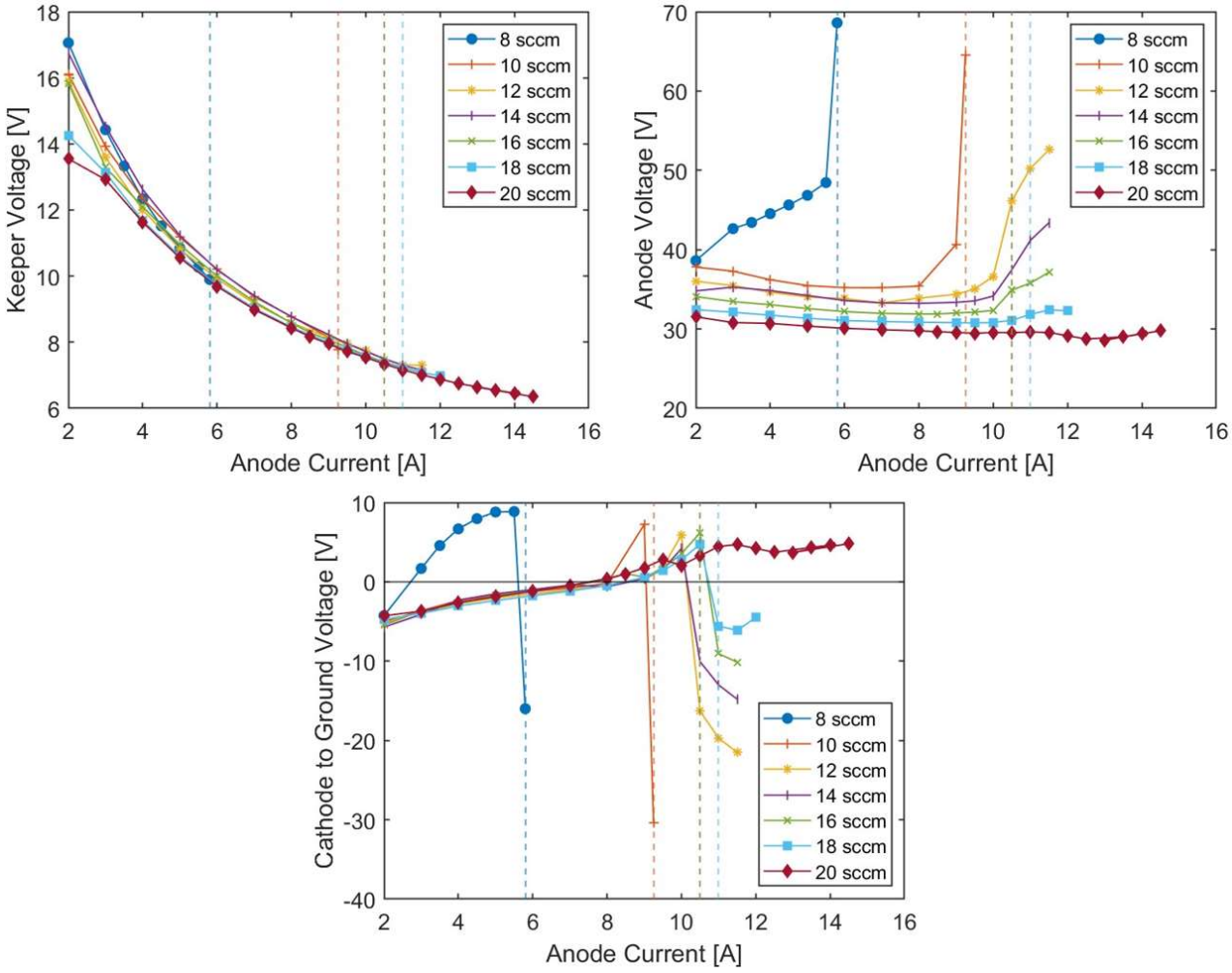

Figure 7: Keeper (top left), anode (top right), and cathode-to-ground (bottom) voltage with respect to anode current for no simulated magnetic field

Subsection 4.1.2 Cathode 1-cm Downstream (DS) of Peak Magnetic Field

Most GIT devices place the hollow cathode downstream of the peak magnetic field, and this test configuration is closest to the standard practice. The keeper, anode, and cathode-to-ground voltage as a function of anode current are shown in Figure 8. The transition point where the anode voltage suddenly increases and coupling voltage decreases is easy to spot and comparable with the data with no simulated magnetic field at lower flow rates of 8 and 10 sccm. At flowrates of 12-20 sccm it is inconclusive whether the transition occurs from observations of the anode and coupling voltage, but the signature of the coupling voltage rising close to zero and then falling at

higher currents is present. It was also difficult to tell visually during the tests with an applied magnetic field whether a transition point had been achieved over the anode current range that was initially studied. The scope traces at higher flow rates also did not indicate conclusive evidence that a transition point had occurred at flowrates of 12 sccm and higher. Another detail to note is that the cathode coupling voltage never goes positive in the tests with an applied permanent magnetic field, unlike the test when no simulated magnetic field was applied.

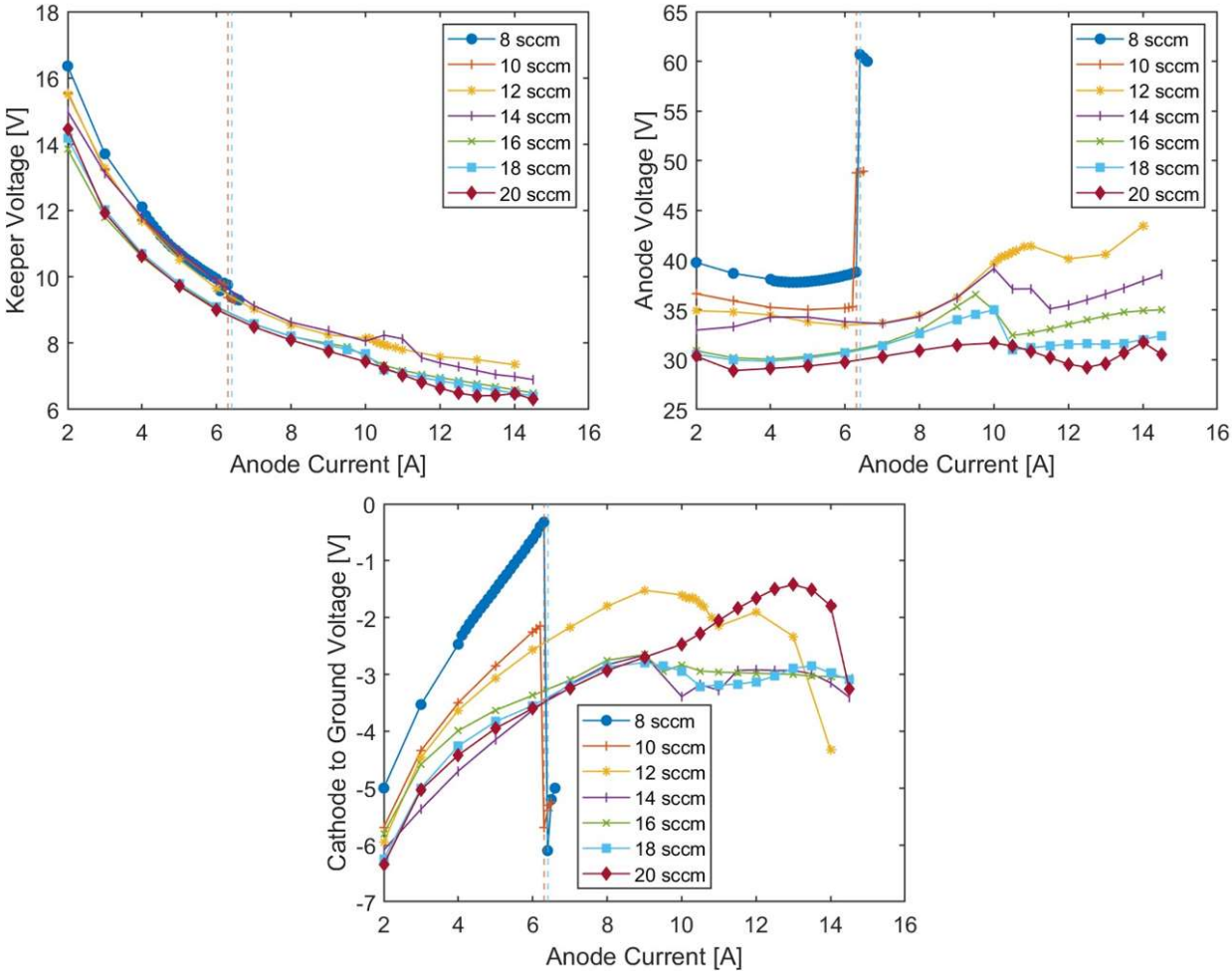

Figure 8: Keeper (top left), anode (top right), and cathode-to-ground (bottom) voltage with respect to anode current for the cathode tip 1-cm downstream of peak magnetic field

Subsection 4.1.3 Cathode 1-cm Upstream (US) of Peak Magnetic Field

As mentioned above, the standard practice in GITs is to place the cathode downstream of the peak field. This test configuration evaluates a cathode placed upstream of the peak field. It is believed to be harder for electrons to couple to the anode when the cathode is upstream of the peak, and we expected that the voltages for this cathode location would be larger and that the mode transitions might occur at lower anode currents. The keeper, anode, and cathode-to-ground voltages with respect to anode current are shown in Figure 9. The keeper voltages decreased with increasing anode current like the previous test configurations. The anode and cathode-to-ground voltages also behaved as in the other tests when the cathode plume transitioned from "quiescent" to "noisy," but the transition was harder to spot at the 8 and 10 sccm flow rates in the anode voltage plots compared to the case with the cathode located downstream of the peak field. The anode voltages were higher for this cathode location, which aligns with our expectation about cathodes placed upstream of the peak field. In the cathode-to-ground voltages, the decrease in voltage is more noticeable at anode currents above the transition. Overall, this magnet configuration visually appeared more unstable than the other configurations, indicating that a forward-shifted peak magnetic field is not a desirable configuration.

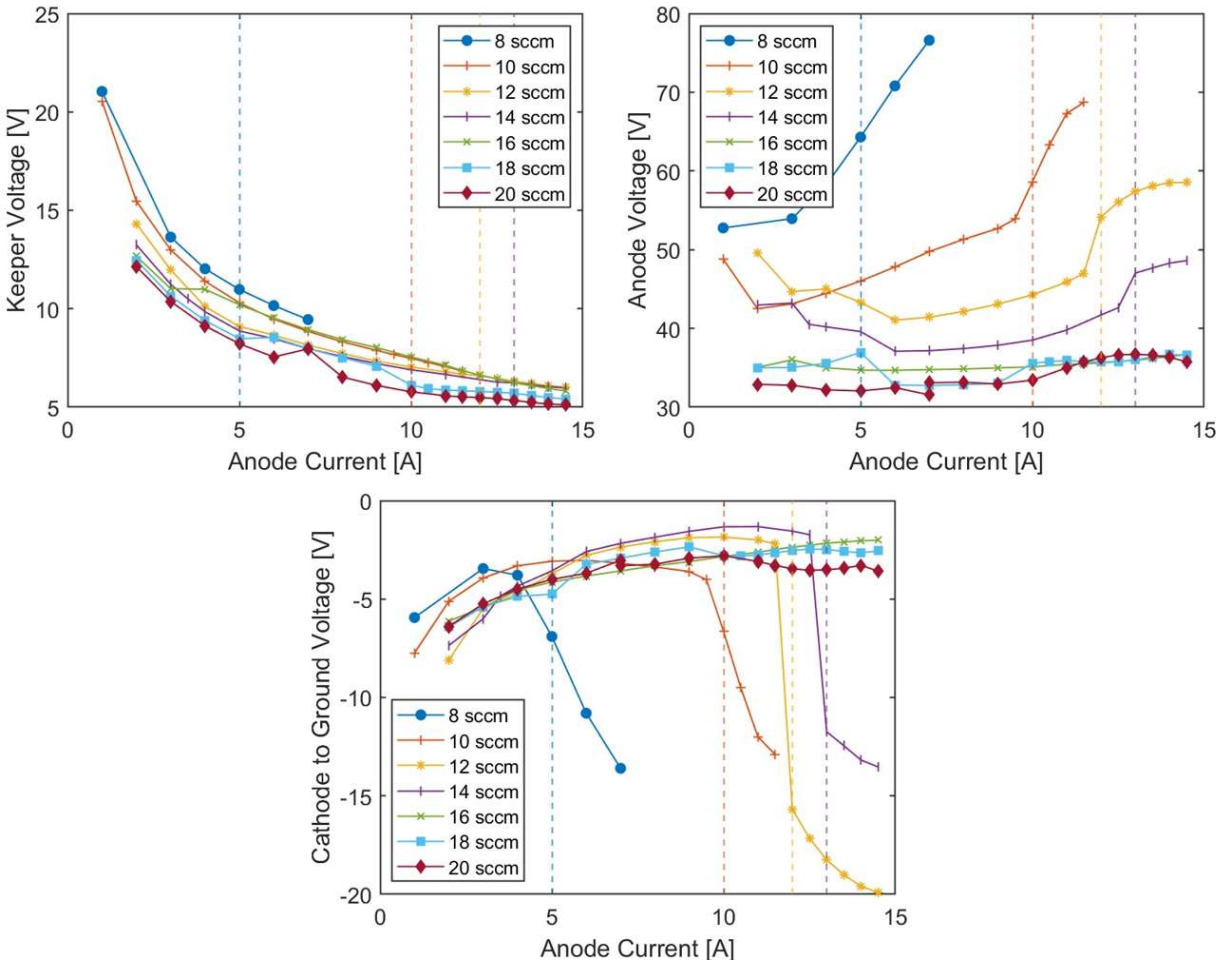

Figure 9: Keeper (top left), anode (top right), and cathode-to-ground (bottom) voltage with respect to anode current for cathode orifice mounted 1-cm upstream of peak magnetic field

Subsection 4.1.4 Cathode at Peak Magnetic Field

Finally, the cathode orifice was mounted at the peak magnetic field location, and its keeper, anode, and cathode-to-ground voltages with respect to anode current are shown in Figure 10. Once again, a transition point can be seen where anode voltage increases and cathode-to-ground voltage magnitude increases. Interestingly, this magnetic field configuration shows the most noticeable change in keeper voltage, which decreases at the transition point, while in previous tests the keeper voltage did not show any variation at all. This cathode location results in the most visually stable operating conditions at anode currents below the transition.

Overall, the anode voltage for higher flow rates increases up to a certain anode current, then gradually decrease and increase again. The cathode coupling voltage with increasing anode current at higher flows is seen to increase, decrease, then decrease slowly or drastically depending on the flow rate. Similar to the previous test, the keeper voltage does not seem to be largely affected by the transition point but shows some more drastic changes at the points where anode and coupling voltage decrease, which may warrant further investigations.

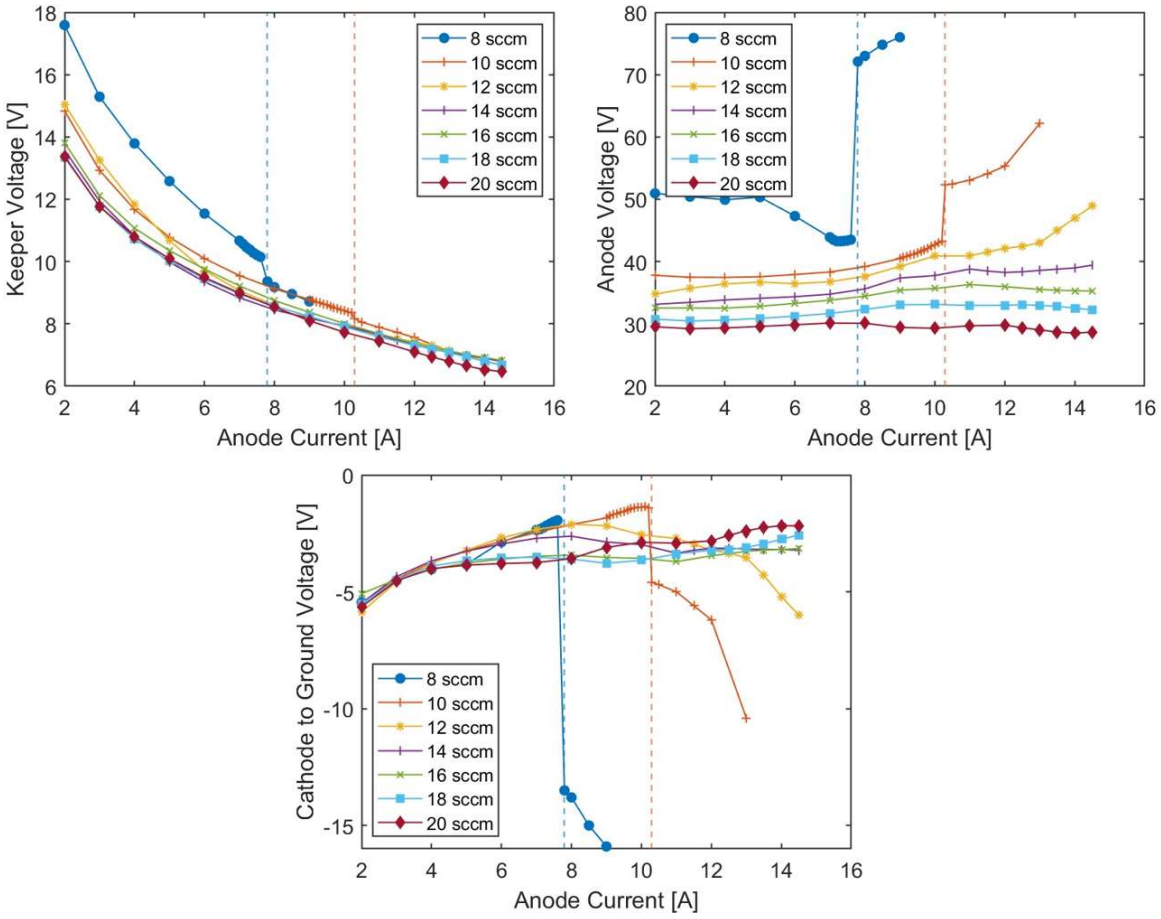

Figure 10: Keeper (top left), anode (top right), and cathode-to-ground (bottom) voltage with respect to anode current for cathode orifice mounted at peak magnetic field

Section 4.2 Permanent Magnet with Cathode at the Peak Field Location (2A-25A)

As the transition from "quiescent" to "noisy" mode tended to only happen with the lower flow rates, a power supply with a higher current limit was used to see if similar behavior would occur with the higher flow rates at higher currents. This testing was performed with the cathode tip located at the peak magnetic field as that was the more stable operating configuration from the aforementioned tests. Plasma potential was measured using an emissive probe, and data acquisition was performed with a data logger. Because this data acquisition method results in more variable raw data, the figures were constructed by averaging five raw data points at each operating condition. Some higher current testing would cause disturbances in the DAQ communication, causing some data to be unobtainable at higher currents. The keeper voltage DAQ malfunctioned during this test; therefore, only the anode, cathode-to-ground, plasma potential, and cold probe voltages are shown in Figure 11. No strong conclusions can be drawn from data collected over a larger anode current range that were not pointed out above for this condition tested over a smaller anode current range.

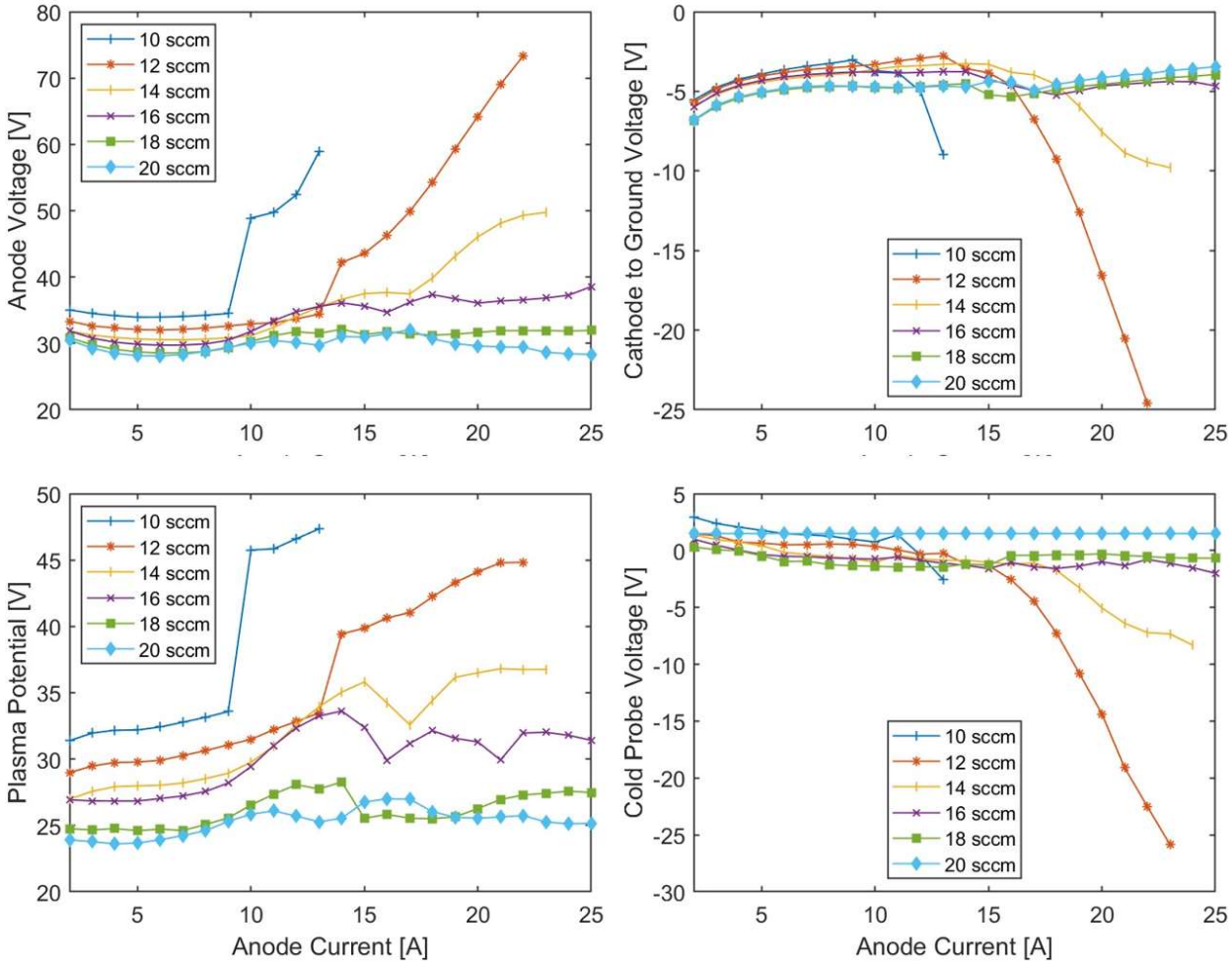

Figure 11: Anode voltage (top left), cathode-to-ground voltage (top right), plasma potential (bottom left), and cold probe voltage (bottom right) with respect to anode current

Subsection 4.2.1 Hysteresis

Some differences in the transition behavior were noted as data were collected with very slowly increasing and decreasing anode current. An example of this is shown for 10 sccm at the cathode orifice mounted 1cm downstream of the peak magnetic field in Figure 12, where a transition while increasing anode current is observed at 6.3A, but the transition back to its original state while decreasing anode current is observed at 4.9A. Another example for 8sccm at the cathode orifice mounted at peak magnetic field location is shown in Figure 13. While increasing anode current, a transition was observed at 7.8A, but when decreasing anode current

from 9A to 2A, the discharge does not appear to transition back to its original "quiescent" state. Data points were taken at 2-minute increments to minimize any temperature transient differences that may have been caused by increasing or decreasing anode current. At the present time we are not able to provide an explanation of the hysteresis behavior or speculate if hysteresis would be expected in thruster testing.

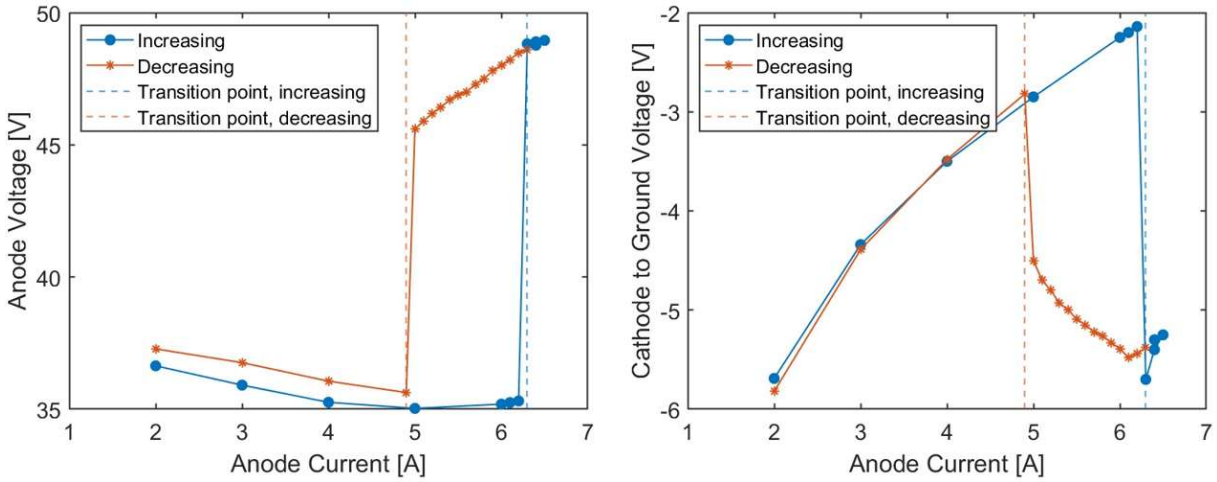

Figure 12: Anode (left) and cathode-to-ground (right) voltage with respect to anode current for 10 sccm at the cathode orifice mounted 1-cm downstream of the peak magnetic field.

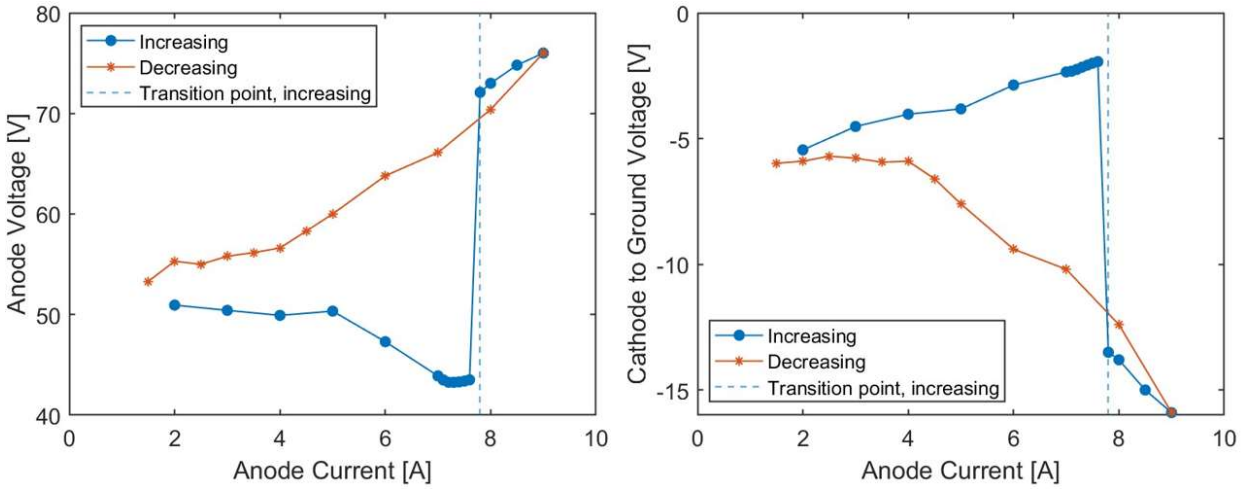

Figure 13: Anode (left) and cathode-to-ground (right) voltage with respect to anode current increasing and decreasing for 8 sccm at the peak magnetic field location

Section 4.3 Solenoidal Magnet (2A-25A)

Keeper, anode, and cathode-to-ground voltages for solenoidal magnetic field testing are shown in Figure 14, while the plasma potential and cold probe voltages are shown in Figure 15. The floating potential of the cold and hot emissive probe is measured relative to facility ground. With the addition of the solenoidal magnet, the 8sccm and 10sccm conditions were visually already in the plume mode at the 2A anode current, while the 12sccm and above data were more inconclusive. Due to the early transition onset, all measurements were noisier than expected and communications for the DAQ system were frequently disrupted at lower flow rate operating conditions.

Keeper voltage decreases with anode current in a manner consistent with previous tests. Anode voltage increases more in this test configuration after the transition to plume mode occurs. Cathode-to-ground voltage increase before decreasing drastically, and similar to the no magnetic field tests, the potential actually goes positive at lower anode currents and flow rates for anode currents below the transition. Plasma potential generally increases, but some flow rates show drops in plasma potential before increasing again. Cold probe voltage continuously decreases with increasing anode current. The increasing differences in the floating voltages of the hot and cold probe state suggest that the electron temperature of the plasma within the anode is increasing with increasing anode current. Visually, the plume of the cathode with the solenoidal magnet is more constrained along the centerline than the other tests and more similar to its appearance while operating with a HT, which could be due to the less divergent structure of the coil magnetic field compared to the permanent magnet ring field structure.

Subsection 4.3.1 RPA Traces

An RPA trace comparison between an operating point before and after the transition to plume mode is shown in Figure 16. Note that this anode potential is with respect to ground instead of with respect to cathode potential. Even with the increase in anode voltage in the transition regime, the most probable energy seems to lower in the transition, which may indicate that data points are being lost to electrons being attracted to the RPA. It is also noteworthy that after the transition, there is a noticeable increase in the presence of higher energy ions compared with that in the quieter mode of operation. It is also possible that the higher peak is not due to the anode, but instead to an increased number of charge exchange ions in the plume state.

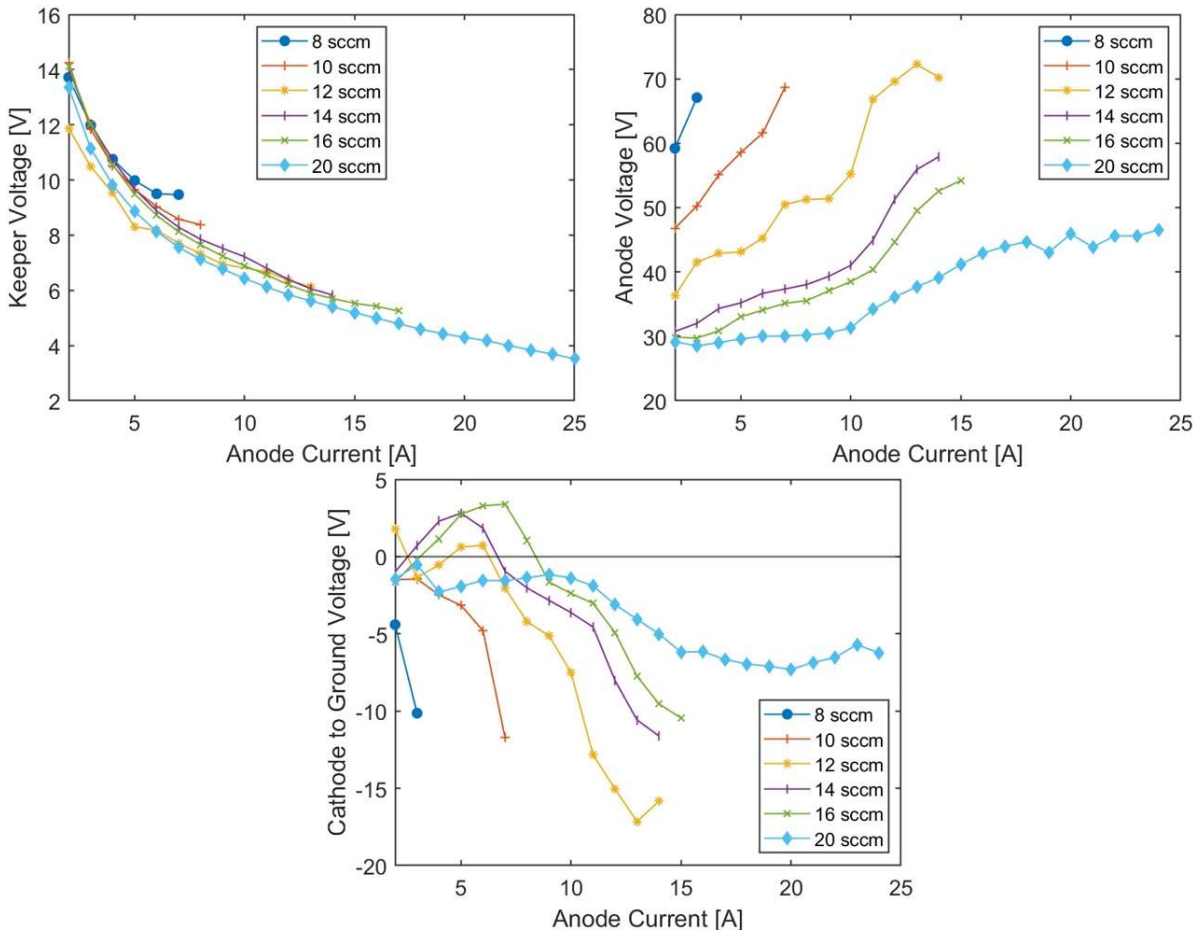

Figure 14: Keeper voltage (top left), anode voltage (top right), and cathode-to-ground voltage (bottom) for solenoidal magnet testing

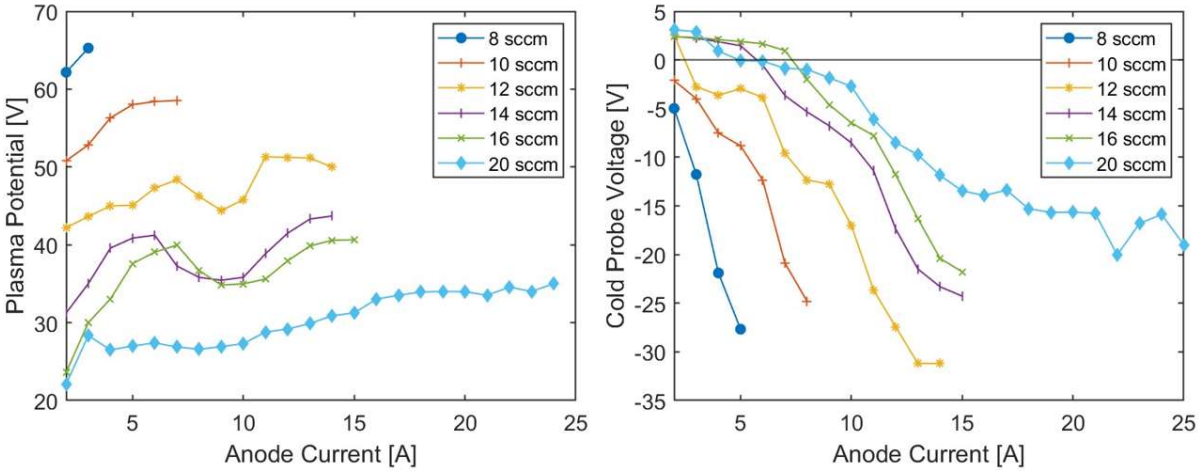

Figure 15: Plasma potential (left) and cold probe voltage (right) for solenoidal magnet

Table 2: Most probable energy, anode voltage, and full width half maximum

I_A [A]	emp [eV]	VA [V]	FWHM [eV]
5	120	43.85	100
8	54	47.44	27

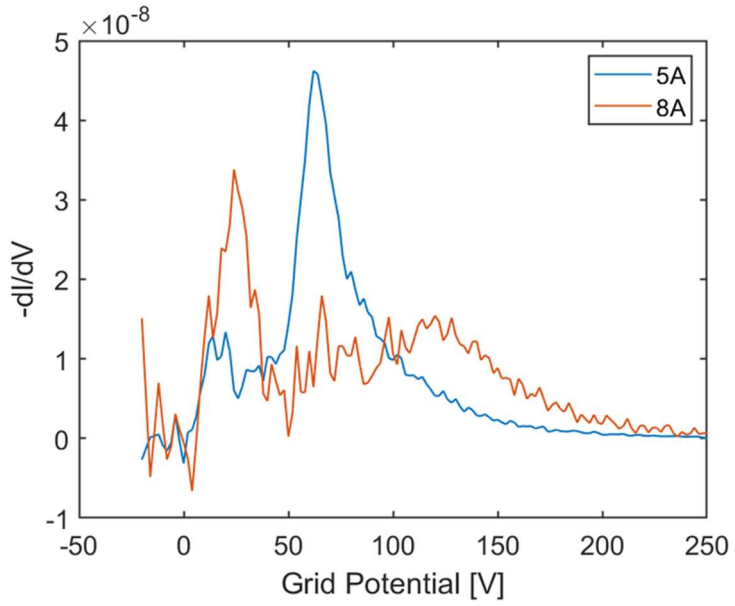

Figure 16: RPA trace for 12sccm, 5A and 8A conditions

Subsection 4.3.2 Oscilloscope Magnitudes

Oscilloscope traces for keeper, anode, cathode-to-ground, and probe voltage were taken at each operating condition. In general, it is seen that at the anode current where the mode transition occurs, oscillation magnitudes increase drastically by >1.4x in keeper, anode, cathode coupling, and plasma potential voltage from the previous operating point taken at an anode current below the transition.

Section 4.4 No Magnetic Field (2A-25A)

Tests were repeated at the no magnetic field configuration over a higher anode current range similar to the tests with the permanent magnet ring. Keeper, anode, and cathode-to-ground voltages are shown in Figure 18, while plasma potential and cold probe measurements are shown in Figure 19. The transition for this test is much more visibly noticeable than that of the permanent magnet ring and the solenoidal magnet coil. During the transition and at higher anode current, the whole chamber is noticeably brighter and DAQ communications oftentimes fail, making it easier to spot when a transition is happening than in previous tests. The cathode-to-ground voltage increases above zero before decreasing dramatically at the transition onset similar to the earlier 'no applied field' condition tested over a smaller anode current range. At higher flow rates, the plasma potential and cold probe voltage both drop at currents above the transition, indicating that those decreases can also flag when a plume mode transition has occurred. The transitions to plume mode also happen at higher currents than that of the previous no magnetic field test, which we do not presently have an explanation for except to point out that very few tests were repeated over and over to build up a statistical prediction of what anode current a transition could be expected to occur at.

RPA traces for operating conditions in plume mode are noisy due to a higher than desired number of electrons getting to the RPA collector; therefore, an RPA trace of an operating point in spot mode and right before plume mode onset are shown in Figure 17. The most probable energy is higher near the plume transition, which corresponds to the higher plasma potential detected there, and more noise is evident in the high energy ion region.

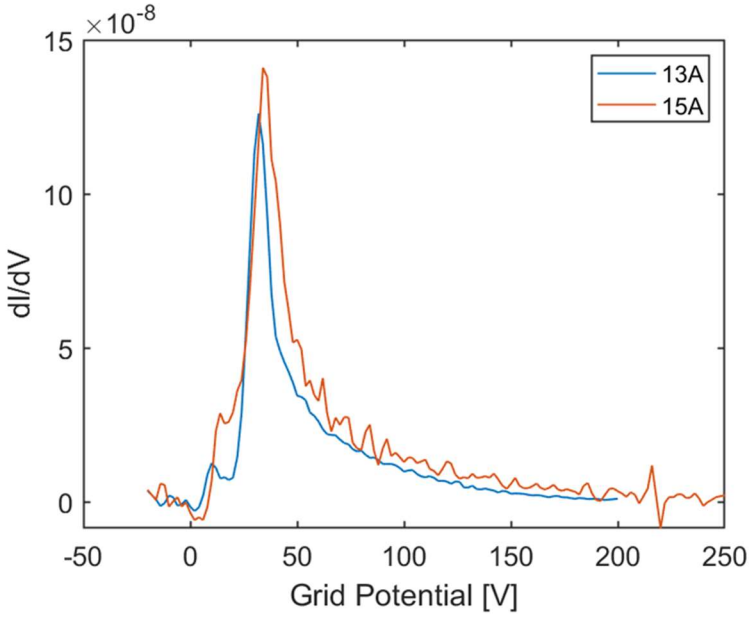

Figure 17: RPA trace of 20sccm, 13A and 15A conditions

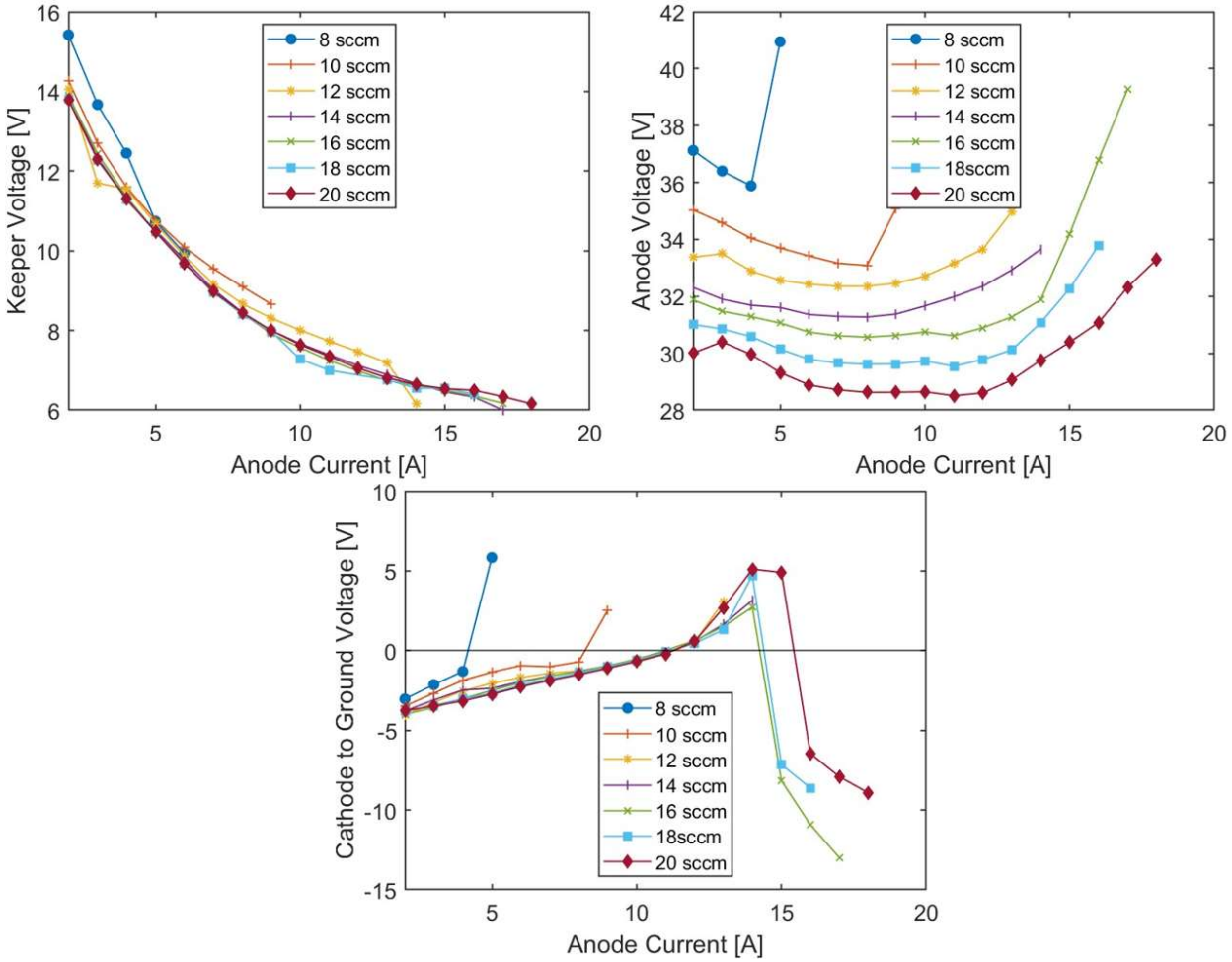

Figure 18: Keeper voltage (top left), anode voltage (top right), and cathode-to-ground voltage (bottom) for no magnetic field testing

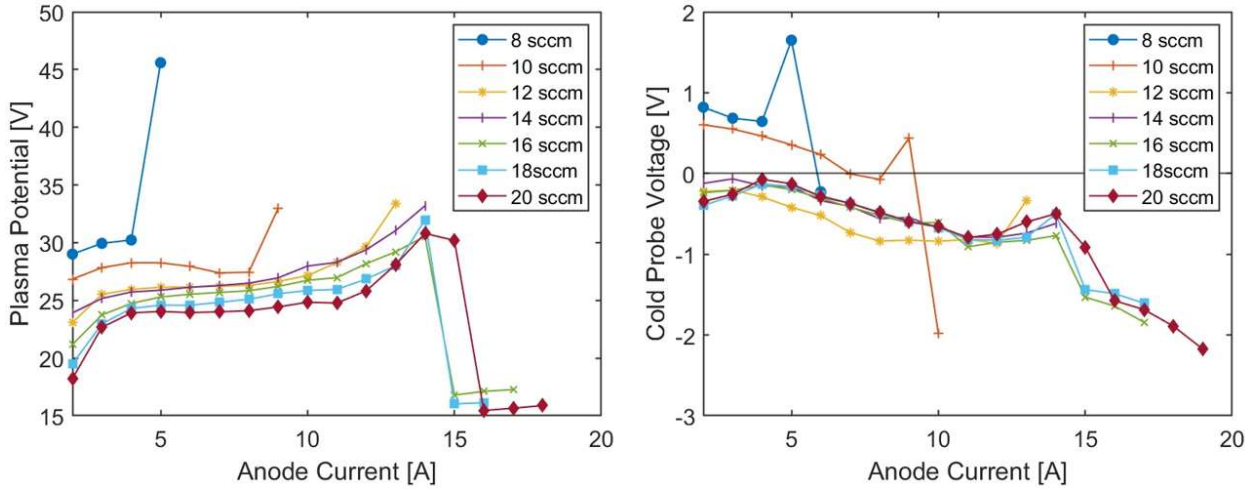

Figure 19: Plasma potential (left) and cold probe voltage (right) for no magnetic field testing.

CHAPTER 5: DISCUSSION

Section 5.1 Spot to Plume Mode Transition

In most tests where anode current was slowly increased, a transition from a "quiescent" mode of operation to a more "noisy" mode was observed. This was marked by an increase in voltage oscillations, increase in anode voltage, and decrease in cathode-to-ground voltage. It can also be seen that the transition corresponds to an increase in plasma potential and the beginning of a steady decrease in cold probe voltage (suggesting electron temperature is increasing). The phenomenon of discharge transition is often referred to in literature as the "spot" to "plume" mode or "quiescent" to "noisy" mode transition. Some literature also refers to a separate mode of operation called the "jet" mode, where the plume appears axially collineated, and a luminous "jet" forms in the center axis of the plume [15, 16]. It is unclear whether the transition we are seeing with applied magnetic field is “spot-to-plume” or “spot-to-jet”, but the visual observations suggest a transition to "jet" mode. The voltage oscillation magnitudes also increase by a factor of >1.4 for keeper, anode, cathode-to-ground, and plasma potential during the transition.

A comparison of the different transition points for different tests are shown in Figure 20, with PM representing permanent magnet, SM representing solenoidal magnet, DS meaning downstream and US meaning upstream. One test with no magnetic field was performed at the very beginning denoted by “No magnetic field – 1”, while another one was performed at the very end of all the other tests, denoted by “No magnetic field – 2.” The solenoidal magnetic field has the lowest flow rate to anode current transition trend, while the second test with no magnetic field has the highest flow rate to anode current transition trend. The solenoidal magnet test has noticeably higher flow rates and lower currents when it transitions, which is consistent with the fact that at lower flow rates at 8sccm and 10sccm, the cathode plume had already transitioned to

plume mode at the 2A and 3A anode current conditions. Currently, we do not fully understand why different results were obtained in the no magnetic field tests. Although all testing was done on Ar, we are concerned with the results obtained with the solenoidal configuration as the solenoidal magnetic field is the closest field to that of a Hall thruster, this could have further implications on thruster operation and the likelihood of a plume mode being onset in thruster testing.

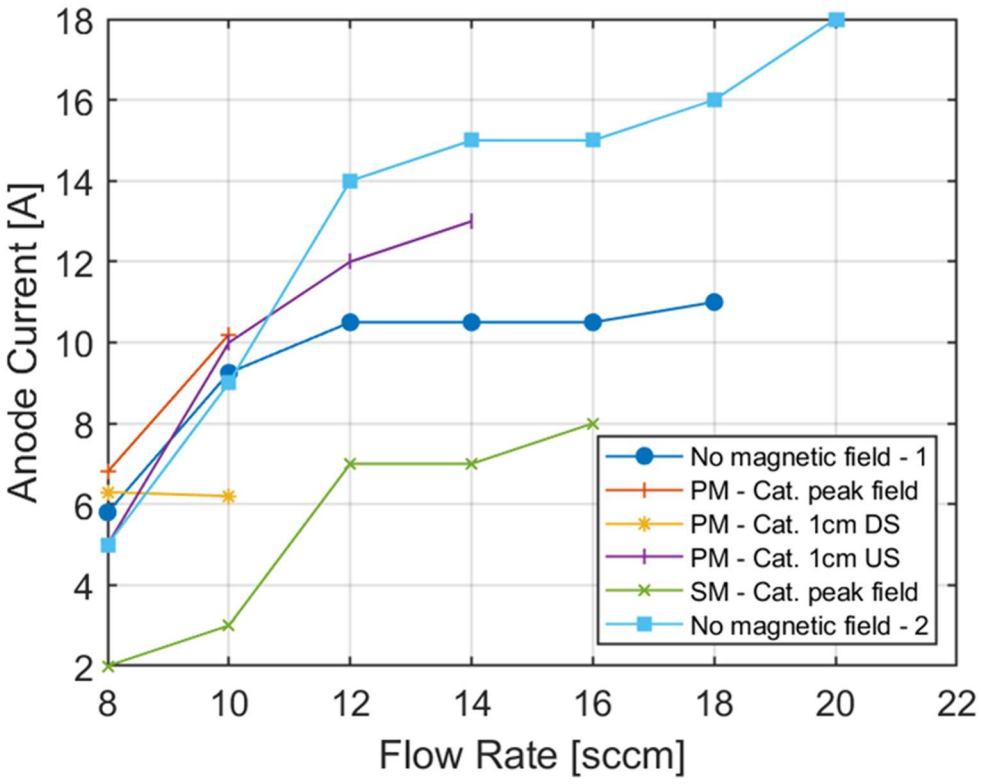

Figure 20: Flow rate and anode current for the transition points of the different tests

Section 5.2 Cathode Coupling Voltage

Without a simulated magnetic field, cathode coupling voltage often goes positive before transitioning to the noisy state, a pattern also observed in the cathode-to-ground voltage during

solenoidal magnetic field testing. However, the cathode-to-ground voltage never rises above zero for the permanent magnetic field testing, regardless of the location of the cathode orifice relative to the permanent magnetic field. Cathode-to-plasma potentials were always negative as expected. It would be interesting to drop cathode flowrate during thruster testing, to determine if cathode potential can bias positive of the chamber wall. Further monitoring of the cathode-to-ground voltage and cathode to plasma voltage in a full thruster test is suggested for future work.

Section 5.3 Hysteresis

We observed that the transition points differ in taking data while increasing or decreasing the anode current, indicating the presence of hysteresis. Oftentimes, the cathode will stay in the "noisy" mode of operation when the anode current has been lowered below the up-swing transition point. This difference in transition anode current would be interesting to study in HT testing especially since in some HTs, the discharge current rapidly oscillates above and below the transition currents observed in this study.

Section 5.4 No Simulated Magnetic Field Tests

Even though two experiments were run with no simulated magnetic field, the transition behavior differs significantly between the very first test run and the second test after the solenoidal magnet experiment. As seen in Table 3, the first test shows lower transition anode current, which is more noticeable at higher flowrates. Besides cathode run time, a different power supply was used. It is possible that minor changes with the cathode apparatus cause the transition to happen at different points, or that the transition threshold is more like a range of values rather than at one precise anode current. More studies and more repeated tests are needed to identify the variability of the transition anode current and what changes to the cathode apparatus have the largest effect on mode transition phenomena.

Table 3: Transition current comparison of first and second experiments with no magnetic field

Flow Rate [sccm]	First Test Transition /[A]	Second Test /[A]
8	5.8	6
10	9.25	10
12	10.5	14
14	10.5	16
16	10.5	15
18	11	15
20	13	16

CHAPTER 6: CONCLUSION AND FUTURE STEPS

We have presented data collected on an instant start, heaterless hollow cathode operated in standalone configurations with and without applied magnetic fields. The applied fields that were tested were configured to resemble those produced around the main discharge cathode in a gridded ion thruster (GIT) and a center mounted cathode in a Hall thruster (HT). There are many aspects of a given hollow cathode design that can be evaluated in a standalone configuration. In this work we focused on characterization of the flowrate and anode current where a transition occurs between relatively quiescent operation (referred to as spot mode) and a noisier mode of operation (referred to as plume mode). Important findings from our work include (1) observation of wide uncertainty in anode current where the spot to plume transition occurs, (2) evidence of strong hysteresis in the transition current depending upon whether the anode current is being increased or decreased, and (3) strong, negative impacts of applied magnetic field on the anode current where the transition occurs. More detailed concluding remarks concerning these findings are described below.

We found that applying a GIT-like and HT-like magnetic field to a standalone hollow cathode setup changed the operating conditions dramatically at currents above and below the point where mode transitions occur. In almost all tests conducted in the 8-12 sccm range, we observed a clear transition from "quiescent" to "noisy" mode at a particular anode current via increases in voltage oscillations that correlated with an increase in anode voltage, decrease in cathode-to-ground voltage, and increase in plasma potential. The presence of a permanent magnetic field resulted in the cathode-to-ground voltage always remaining below zero at anode currents above and below mode transitions. However, operating without an applied magnetic field and with a solenoidal magnetic field consistently resulted in the cathode-to-ground voltage

increasing to positive values relative to facility ground just below the anode current that triggered a mode transition to occur. The presence of a permanent magnetic field also causes the mode transition to occur at lower anode currents when a transition was detectable, whereas the solenoidal magnetic field leads to mode transitions at even lower anode currents. This has significant implications for thruster testing which utilizes lower flow rates than the standalone test, indicating that the cathode may be operating close to or within the mode transition region during normal operation. As mentioned above, we observed the cathode potential can bias positive of the vacuum chamber ground in standalone tests and testing with a Hall thruster (HT) at low cathode flows may uncover similar behavior especially in HT operation with a strong breathing mode occurring. In this regard, we point out that hysteresis behavior was observed with the spot-plume transition in all the tests conducted with applied magnetic field. RPA traces show evidence of high energy ions being present at anode currents above the transition for solenoidal magnet testing.

The anode currents triggering mode transition are higher for the second 'no applied magnetic field' test compared to the first test. This could be due to minute changes in the test apparatus (for example, changing out an anode power supply), further emphasizing the need for a standardized cathode testing protocol, which is commented upon more in the text below. Additionally, the differences observed between the first and second test could indicate that the transition behavior of a cathode has larger error margins than previously expected and is not triggered at a specific anode current, but over a wide range of current. The hysteresis observed in our tests further complicates the results of the first and second test with no applied magnetic field, which might include the recommendation of adding of a standard filter circuit between the anode power supply and the cathode and anode electrodes. It is suggested that future testing of

cathodes in standalone configurations be done with a standardized electronic filter placed between the anode power supply and a test article to help remove the effect that power supply output circuits and control loops might have on the tests.

For other future steps, we hope others will compare our data to data collected with a Hall thruster to further document the differences between standalone and thruster testing. This includes monitoring the cathode-to-ground voltage and plasma potential to monitor if the thruster cathode-to-ground voltage indeed biases positive, and if a mode transition can be observed. We also hope to expand this study to higher-current cathodes comparable to those used in the H9 HT. One theory as to why the "quiescent" to "noisy" mode transition happens is that some regions in the cathode plume are being starved of neutrals. To further study the transition period for the cathode, we recommend future work using two-photon absorption laser-induced fluorescence (TALIF) to study the neutral density variation downstream of the cathode, which has recently been demonstrated with Krypton propellant. Finally, a breathing mode is often observed in Hall thrusters that is not observed in standalone hollow cathode tests. An artificial breathing mode simulated with a high-speed anode power supply system is recommended to be used on standalone hollow cathode tests. This would involve oscillating the anode current at frequencies of 5-40 kHz to study how high amplitude anode current fluctuations affect mode transitions and cathode operating conditions.

CHAPTER 7: REFERENCES

[1] Goebel, D. M., and Katz, I., Fundamentals of Electric Propulsion: Ion and Hall Thrusters, JPL Space Science and Technology Series, California Institute of Technology, 2008.

[2] Goebel, D. M., Becatti, G., Mikellides, I. G., and Ortega, A. L., "Plasma hollow cathodes," Journal of Applied Physics, Vol. 130, No. 050902, 2021.

[3] Goebel, D. M., Becatti, G., Mikellides, I. G., and Ortega, A. L., "Plasma hollow cathodes," Journal of Applied Physics, Vol. 130, 2021. https://doi.org/10.1063/5.0051228.

[4] Siegfried, D. E., and Wilbur, P. J., "An Investigation of Mercury Hollow Cathode Phenomena," 13th International Electric Propulsion Conference, 2012. https://doi.org/10.2514/6.1978-705.

[5] Goebel, D. M., Jameson, K. K., Watkins, R. M., et al., "Hollow cathode theory and experiment. I. Plasma characterization using fast miniature scanning probes," J. Appl. Phys, Vol. 98, 2005. https://doi.org/10.1063/1.2135417.

[6] Mikellides, I. G., Guerrero, P., Ortega, A. L., Goebel, D. M., and Polk, J. E., "Investigations of Spot-to-plume Mode Transition in a Hollow Cathode Discharge Using 2-D Axisymmetric Plasma Simulations," 2018 Joint Propulsion Conference, 2018. https://doi.org/10.2514/6.2018-4722.

[7] Potrivitu, G.-C., Xu, L., Levchenko, I., Huang, S., Sun, Y., Wisnuh, M., bin Rohaizat, A., Wei, J., Lim, M., Bazaka, K., and Xu, S., "Mode Transition in a Low-current LaB6 Hollow Cathode for Electric Propulsion Systems for Small Satellites," IEPC, Vol. Plasma Sources and Application Centre/Space Propulsion Centre, Nanyang Technological University, No. Singapore 637616, 2019.

[8] Hall, S. J., Sarver-Verhey, T. R., Frieman, J. D., Kamhawi, H., and Myers, J. L., "Preparation for Hollow Cathode Testing for the Advanced Electric Propulsion System at NASA Glenn Research Center," AIAA/SAE/ASEE Joint Propulsion Conference, ????

[9] Hall, S. J., Gray, T. G., Yim, J. T., Choi, M., Mooney, M. M., Saver-Verhey, T. R., and Kamhawi, H., "The Effect of a Hall Thruster-like Magnetic Field on Operation of a 25-A class Hollow Cathode," 36th International Electric Propulsion Conference, 2019. https://doi.org/20190032078.

[10] Frieman, J. D., Kamhawi, H., Williams, G. J., Huang, W., Herman, D. A., Peterson, P. Y., Gilland, J. H., and Hofer, R. R.,

[11] "Long Duration Wear Test of the NASA HERMeS Hall Thruster," 54th Joint Propulsion Conference cosponsored by AIAA, SAE, and ASEE, 2019. https://doi.org/20180006433.

[12] Hall, S. J., Gray, T. G., Yim, J. T., Choi, M., Saver-Verhey, T. R., and Kamhawi, H., "The effect of facility background pressure on hollow cathode operation," Journal of Applied Physics, Vol. 130, 2021. https://doi.org/https://doi.org/10.1063/5.0061045.

[13] Lai, J.-J., Chen, Q.-M., and Qiu, J.-L., "The effect of various magnetic field configurations on a hollow-cathode discharge," Journal of Applied Physics, Vol. 33, 1999. https://doi.org/10.1088/0022-3727.

[14] Imaguchi, D., Watanabe, H., Imai, S., Funaki, I., and Yamagiwa, Y., "Characterization of a Hollow Cathode Plasma with Magnetic Fields," AIAA Propulsion and Energy Forum, 2021. https://doi.org/10.2514/6.2021-3388.

[15] Ham, R. K., Williams, J., Thompson, S. J., and Farnell, S., "A Low Erosion Instant Start Ignition Process for Heaterless Hollow Cathodes," Space News, Vol. 8, No. 2, 1997, pp. 13–19.

[16] Goebel, D. M., Jameson, K. K., Katz, I., and Mikellides, I. G., "Plasma Potential Behavior and Plume Mode Transitions in Hollow Cathode Discharges," IEPC-2007-277, 2007. https://doi.org/IEPC-2007-277.

[17] Goebel, D. M., Jameson, K. K., Watkins, R. M., and Katz, I., "Hollow Cathode and Keeper-region Plasma Measurements Using Ultra-fast Miniature Scanning Probes," 40th AIAA/ASME/SAE/ASEE Joint Propulsion, 2004. https://doi.org/20070023499.

[18] Antozzi, S., Gottfried, J., Williams, J. D., and Yalin, A. P., "Spatially Resolved Measurements of Krypton by Two-photon Absorption Laser Induced Fluorescence (TALIF) in a Barium Oxide Hollow Cathode Plasma," AIAA 2023-4269 Session: Plasma and Laser Diagnostics I, 2023. https://doi.org/https://doi.org/10.2514/6.2023-4269.

[19] Jenkins, N., "Breathing Mode Effects on Hall Thruster Plasma Quantities and Channel Wall Power Loss," 2019.